Recyclability of 304L Stainless Steel in the Selective Laser Melting Process

Austin T. Sutton[1], Caitlin S. Kriewall[2], Ming C. Leu[1], Joseph W. Newkirk[2]

[1]Department of Mechanical and Aerospace Engineering, Missouri University of Science and
Technology, Rolla, MO 65409
[2]Department of Materials Science and Engineering, Missouri University of Science and
Technology, Rolla, MO 65409

Abstract

During part fabrication by selective laser melting (SLM), a powder-bed fusion process in Additive Manufacturing (AM), a large amount of energy is input from the laser into the melt pool, causing generation of spatter and condensate, both of which have the potential to settle in the surrounding powder-bed compromising its reusability. In this study, 304L stainless steel powder is subjected to five reuses in the SLM process to assess its recyclability through characterization of both powder and mechanical properties. Powder was characterized morphologically by particle size distribution measurements, oxygen content with inert gas fusion analysis, and phase identification by X-ray diffraction. The evolution of powder properties with reuse was also correlated to tensile properties of the as-built material. The results show that reused powder coarsens and accrues more oxygen with each reuse. The effects of powder coarsening and oxygen increase on the tensile properties of fabricated parts are being investigated.

Introduction

Powder-bed fusion is a class of additive manufacturing (AM) methods that bond successive layers of powder to form three-dimensional components directly from computer-aided design (CAD) files. Among the powder-bed fusion techniques is the selective laser melting (SLM) process, which fuses particles together with a laser. Due to the precision of the laser as well as the use of powders which often do not exceed 70 µm in diameter, SLM is able to produce geometrically complex parts with high dimensional accuracy [1]. Since the main consolidation mechanism is through direct melting of powdered material, components manufactured by SLM exhibit high density lessening the need for post-processing [2]. Consequently, SLM has captured the attention of the aeronautical, biomedical, and automotive industries.

While the use of powder as the raw input material in SLM can be challenging due to the need for high flowability and apparent density [3], powders offer several advantages including their ability to act as supporting material during fabrication, ease of mixing for better control of part chemistry, and recyclability. This not only gives flexibility for tailoring powder properties aimed at increasing part performance, but also enables the possibility for generating little material waste compared to conventional subtractive methods for manufacturing components. In SLM, it is common practice to use less than 50% of the build area leaving a substantial amount of material unconsolidated surrounding parts. Since AM-ready powder is expensive due to the need for spherical particles with high purity, the ability to reuse powder can allow for substantial cost

savings making the process more economical. However, it is uncertain whether the powder that has been subjected to the SLM environment can be used for part fabrication without deterioration of part quality.

To understand how powder that is unused in the SLM process can be affected has spurred researchers to investigate the ejecta that occur during fabrication. Collectively, there exist two types of ejecta that are inherent in SLM, namely, laser spatter and condensate, which both settle into the powder-bed surrounding parts. Condensate refers to the material that is vaporized while the laser interacts with the powder-bed, which is a submicron powder that is formed as the vapor cloud above the melt pool is rapidly quenched in the chamber atmosphere [4–6]. If not adequately removed from the path of the laser beam, attenuation of the laser power can occur causing pores to develop in the part [4,5]. Another important consequence of condensate formation stems from the superheated vapor cloud above the melt pool from which it formed. Since the vapor cloud has a substantially different temperature and pressure from the build chamber atmosphere, local pressure-driven flow currents that drag particles from the surrounding powder-bed into the path of the laser beam. While some particles are melted to form the parts, others are heated by the laser and then subsequently ejected leading to spatter. Through simulations, Ly et al. [7] was able to show that while laser spatter in SLM is partially caused by recoil pressure of the melt pool, a large portion is due to the micro-jets near the weld.

Having been ejected after interaction with the melt pool, laser spatter particles differ from the base powder morphologically, chemically, and microstructurally. Studying 316L stainless steel, Al-Si10-Mg, and Ti-6Al-4V laser spatter, Simonelli et al. [8] found that the ejected particles are much larger than the base powder and also contain oxides on their outer surfaces. Liu et al. also concluded that the laser spatter contains abnormally large particles which caused deleterious effects on the tensile properties of components [9]. The authors have also conducted extensive work in characterization of 304L laser spatter where laser spatter was found to be comprised of a wide size distribution from nearly 1 μm to 150 μm. Moreover, oxide islands were observed on the surfaces of laser spatter particles due to solidification in the chamber atmosphere at approximately 1000 ppm oxygen content. Lastly, a unique signature of laser spatter was also revealed with microstructural analysis through x-ray diffraction (XRD) where the laser spatter contains a large volume percentage of delta ferrite compared to the austenitic starting powder [10].

Due to these differences, deposition of laser spatter and condensate in the build area will undoubtedly alter the powder as it is recycled. Therefore, evaluating the recyclability of powder in SLM has been a primary concern for some researchers [11–13]. When studying Ti-6Al-4V in the EBM process, Tang et al. [11] found that the oxygen content of recycled powder increased causing a subsequent increase in the yield and ultimate tensile strength. In regards to the morphology, the size distribution of the used powder tightened and number of satellites decreased causing the powder to have an increase in flowability. After recycling the powder 21 times, it was concluded that no undesirable effects occurred. A similar conclusion was found by Ardila et al. [12] who recycled Inconel 718 in the SLM process to find that the powder coarsened slightly, but did not yield an appreciable influence on the material toughness after 14 reuses. Slotwinski et al. [13] also noticed powder coarsening of both CoCr and 17-4 stainless steel when reused, and found

that the surfaces of recycled powder contain oxides that were not found in either of the virgin powders.

While powder recycling has been performed for many other materials, the effects of reusing austenitic stainless steels in SLM on the part properties is seldom in the literature. Therefore, the goal of this paper is to subject 304L powder to multiple reuses in SLM and evaluate the properties of the parts built with each use of powder. While the powder is studied with respect to its morphology, chemistry, and microstructure, the mechanical performance of manufactured parts is evaluated by observing the trend in tensile properties for appreciable differences due to powder variation.

Experimental Methods

The goal of the recycling study presented in this paper is to thoroughly validate the recyclability of 304L stainless steel in the SLM process when subjected to a worst-case scenario aimed at accelerating powder degradation through successive reuse. One of the methods by which this was accomplished was by using only a single batch of powder without replenishing the consumed material in each build with virgin powder. Therefore, the recycled powder was not mixed with virgin powder since such a procedure could extend its reusability. Rather, the height of the build was subsequently decreased after every powder reuse to accommodate for powder loss up to a total of 5 iterations starting from the 0th iteration, where iteration 0 corresponds to using virgin 304L material. Therefore, the parts of the 0th iteration build were oversized by 35 mm in the building direction to accommodate 5 future iterations. Since powder recyclability also depends on the amount of laser spatter and condensate that deposits in the powder-bed surrounding parts, powder degradation also varies with the amount of material being selectively melted in each layer. This was demonstrated by Kriewall et al. [14] who varied the amount of area melted on the build plate to ultimately find that increasing the amount of area selectively melted led to more coarsening of recycled powder. Although increasing the fraction of the build area melted will cause powder degradation to occur at a faster rate, the time needed to build the parts in addition to the amount of powder consumed also increases. In order to reduce the time needed for manufacturing as well as maintain a sufficient amount of powder for use continual reuse, approximately 35% of the build area was utilized as this was deemed sufficient based on the experience of the authors.

Figure 1 shows the build designed for this study which was built by a Renishaw AM250. The parts built include 7 square columns for extraction of mini-tensile specimens with a Sodick VZ300L Wired EDM, 36 Charpy specimens built at a 45° angle, and hollow cubes for measuring powder-bed density. The AM250 is equipped with a 200W Nd-YAG pulsed laser with a wavelength of 1070 nm and a Gaussian beam intensity profile. Prior to processing any parts, the build chamber was stabilized with an oxygen content of < 1000 ppm. A constant 400 ft³/min volumetric flow rate of argon crossflow was maintained across the build area during operation to serve as the shielding gas and to provide removal of melt pool ejecta from the laser beam path. The substrate temperature was held at 80°C. The powder used in this study was gas-atomized 304L stainless steel purchased from LPW Technology with the chemical composition listed in Table 1.
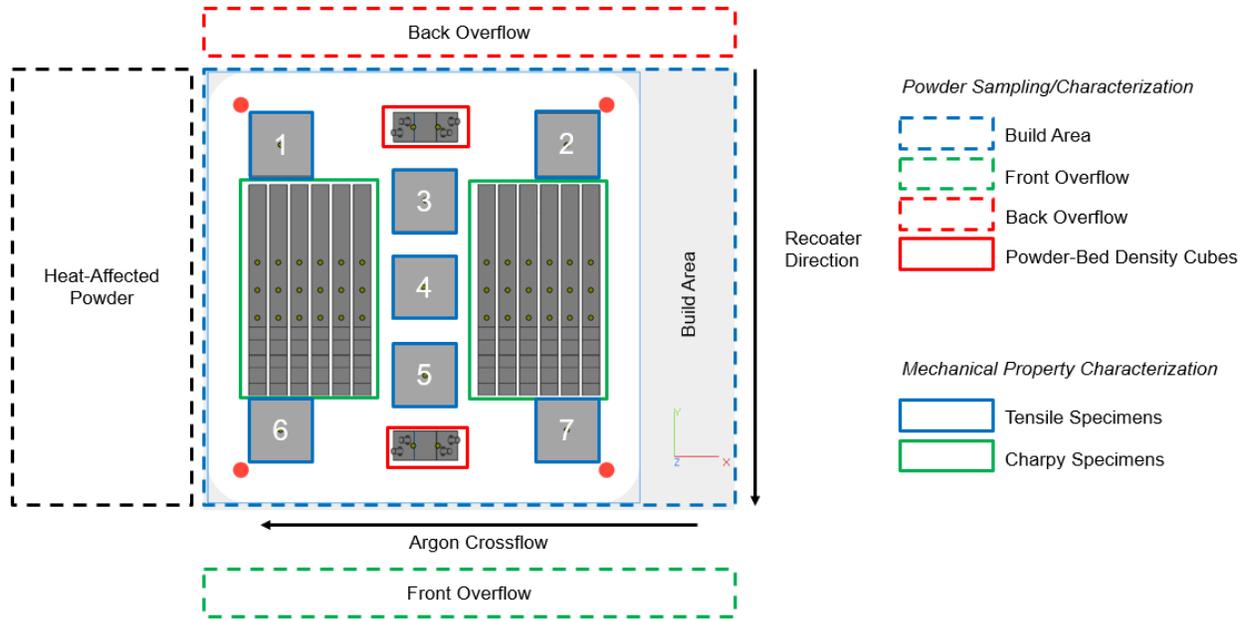
Figure 1: Illustration of build layout highlighting the regions where powder was sampled and the locations of both tensile and Charpy specimens on the build plate. The amount of area used on the build plate is approximately 35%.

Table 1: Chemical composition of unused 304L stainless steel powder

Element	C	Cr	Cu	Fe	Mn	N	Ni	O	P	S	Si
Wt %	0.018	18.4	< 0.1	Bal	1.4	0.06	9.8	0.02	0.012	0.005	0.6

Also shown in Figure 1 are the sampling locations of both the powder and parts for characterization. Five samples of powder were collected from four locations after each iteration, namely, the front overflow and back overflows where excess powder was swept in each layer, build area, and an area downstream of the build area rich in laser spatter and condensate ejected from the melt pool, also known as heat-affected powder. Once samples were extracted, all excess powder after each build was sieved at 63 µm and placed directly back into the AM250 for subsequent reuse. To track the properties of the powder being inserted into the AM250, three additional powder samples were taken after the powder was sieved at 63 µm. While additional powder characterization in the future will analyze all powder samples collected, the work presented in this paper focuses on the size distribution and oxygen content of the powder that is sieved below 63 µm. Prior to all characterization, the powder was homogenized with a Turbula Mixer to minimize sampling bias. All particle size measurements were obtained through an ASPEX 1020 scanning electron microscope (SEM). Sample preparation involved sprinkling 304L powder on a carbon dot atop a blank bakelite mount. The sample was then electrically grounded with copper tape to minimize charging and drifting artifacts. Rather than manually capture images of all prepared powder samples, the ASPEX 1020 SEM is equipped with an automated data collection procedure known as Automated Feature Analysis (AFA). AFA is a unique feature of the ASPEX that analyzes pre-determined areas of a sample for particles with respect to their

projected area and perimeter as well as chemistry through EDS measurements. Using the measured projected area of each particle, the equivalent diameter was computed assuming a perfect circle. To ensure that an adequate number of particles were analyzed for generation of number distributions [15], 3 separate samples of each powder sample were analyzed yielding a minimum of 15,000 particles when combined.

The oxygen content of the sieved -63 µm powder was measured through inert gas fusion with a LECO TC-500 at each iteration of the study. For each iteration, the oxygen content of 3 samples was determined. Prior to measurement, the instrument was calibrated to ensure that the data was reliable with standards that were both above and below the oxygen content of each sample. Sample preparation involved placing the powder inside a tin capsule, which was then placed inside a nickel basket. The nickel basket was then inserted into a graphite crucible before placement into the instrument. To correct for oxygen within the graphite crucible, nickel basket, and tin capsule, the oxygen content of 3 samples without powder were measured and the average oxygen content was subtracted from all samples containing powder.

To determine if the microstructure of the powder changed after continual reuse, powder samples of iterations 0 and 5 which had passed through a -63 µm mesh screen were tested with x-ray diffraction (XRD). Using a Panalytical X'Pert Pro Multi-Purpose Diffractometer X-Ray Diffraction instrument, the phases within both samples were obtained within the 2θ range of 40°-100° over a period of 3 hours. RIQAS 4 software was then used to quantify the volume percentages of the phases present through Rietveld refinement.

While both mini-tensile and Charpy specimens were manufactured, mini-tensile properties are only reported in this paper for quantifying possible mechanical behavior changes due to evolving powder characteristics. Figure 2 is a drawing of the mini-tensile specimen used in this study, which was developed at Missouri University of Science and Technology and have a thickness of 1 mm. Prior to testing, all specimens were polished with 600 grit SiC paper. All tensile testing was carried out on an Instron UTM with custom self-aligning wedge grips to ensure that each specimen was pulled uniaxially. The specimens were pulled at a strain rate of 0.015 mm/min until yield, and then afterwards at 0.5 mm/min until failure. Of the 7 columns available, mini-
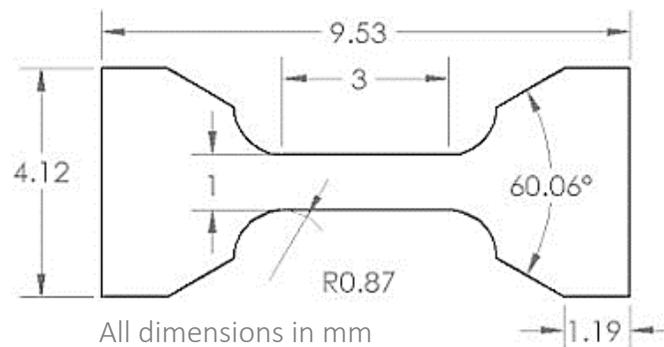

Figure 2: Dimensions of the mini-tensile specimen used in the current recycling study. At least 20 individual specimens were tested from 3 different locations for each iteration equating to a total of 388 total tensile tests.

tensile specimens were extracted from locations 1, 4, and 7. At least 20 MT2 specimens were extracted from each location for each of the 6 builds giving a total of 388 tensile tests. For testing of statistical significance, all tensile test results were input into Minitab where an ANOVA and Tukey analyses with significance levels of 0.05 were used.

Results and Discussion

The primary goal of this paper is to quantify possible changes in the tensile properties of 304L material manufactured by SLM when using powder that was subjected to multiple reuses. Therefore, the results presented herein are split into two subsections with one focusing on the characterization of powder as it is recycled and the other highlighting any differences in part properties.

Powder Characterization

Particle size distributions of various locations for Iteration 0 are shown in Figure 3 with each distribution consisting of at least 15,000 particles. It should be noted that the Iteration 0 -63 µm powder sample represents virgin 304L powder that is sieved prior to insertion into the AM250. Since particle sizes were measured directly with a SEM, the distributions shown are on a number basis. While number distributions can be converted to volumetric, the authors refrained from such a procedure since volumetric distributions often misrepresent the number of fines present. Also
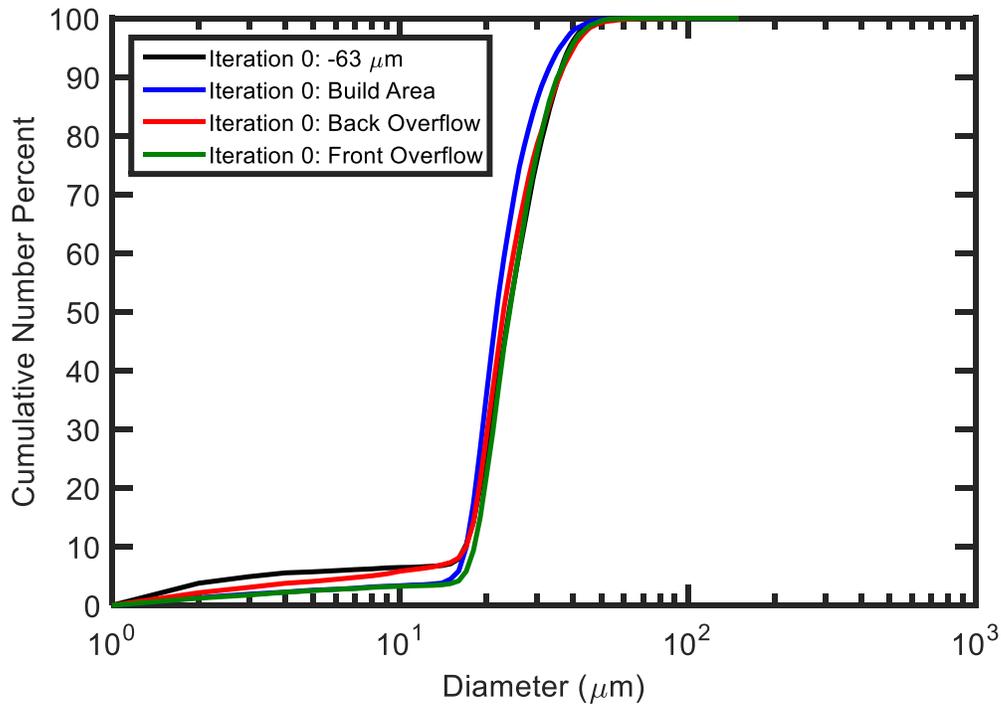

Figure 3: Numeric particle size distributions for powder collected from various locations for Iteration 0.

noteworthy was the decrease in the number of fines for all of the other distributions seen with the front overflow having the least amount of particles less than 15 µm.

Table 2: Tabulated D10, D50, and D90 values of the particle size pertaining to the analyzed powder samples of Iteration 0 at various locations in the AM250. The build area and the back overflow are seen to contain the largest particles indicating the presence of laser spatter.

	-63 µm	Build Area	Back Overflow	Front Overflow
D10	16.8	17.0	17.0	18.1
D50	23.9	21.6	22.9	24.0
D90	35.6	32.0	35.8	35.3
Maximum	70.0	126	121	67.3

Attention should be drawn to the difference in the distributions when considering the front and back overflows where the back overflow is coarser than the front. Observing that the maximum particle size detected in the back overflow was nearly 120 µm as compared to the 67 µm in the front (Table 2) suggests that laser spatter particles were swept into the back overflow after the completion of each layer where the recoater went back to its home position in preparation for spreading of the next layer. These results also indicate that there was a large amount of powder segregation that occurs as a result of the SLM process with respect to the location that the unmelted
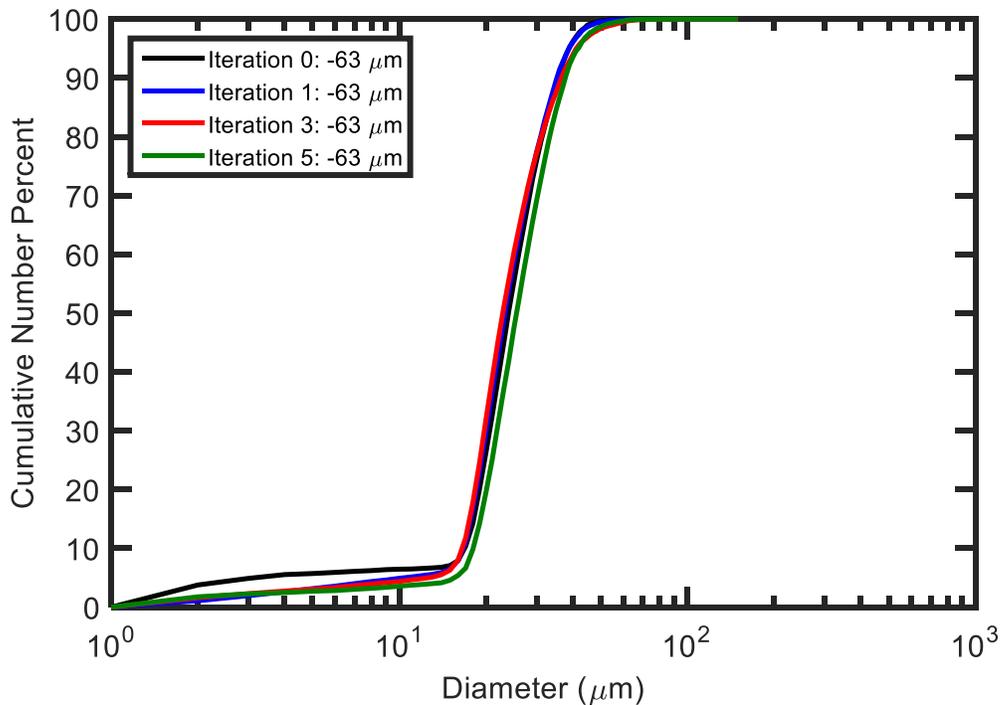

Figure 4: Numeric particle size distributions for powder collected from various iterations throughout the recycling study. It is seen that the number of fines decreases as the powder is recycled in the SLM process.
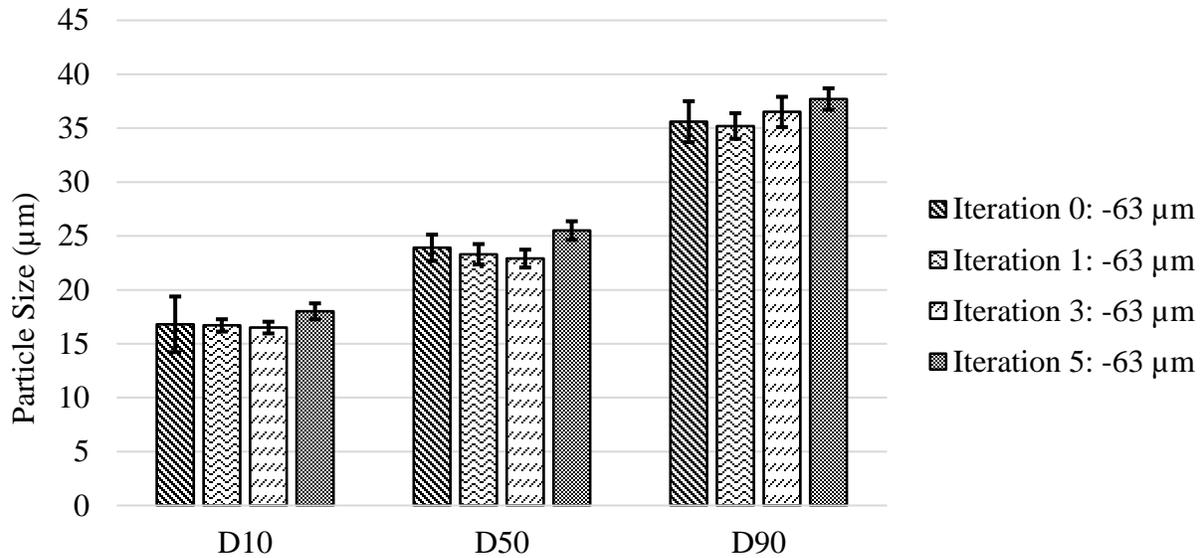
Figure 5: 10th, 50th, and 90th percentiles for each of the powder samples inserted into the AM250 at each iteration in the recycling study. Slight powder coarsening is noticed especially in the 5th iteration.

powder was deposited. This result implies that homogenizing, or thoroughly mixing, powder after sieving in preparation for building parts may be necessary to minimize the variability in part properties.

Particle size distributions of sieved powder sampled before it was inserted into the AM250 are shown in Figure 4. It is important to note that the distributions shown are the combination of 3 individual samples to increase the reliability of the data. For ease of comparison, Figure 5 compares the D10, D50, and D90 of the -63 µm distributions plotted in Figure 4 with corresponding standard deviations being computed from the three samples analyzed from each iteration. While the D10, D50, and D90 of each iteration are similar, the D90 values were gradually increasing with iteration. Moreover, the cumulative percentiles of the 5th iteration were the largest indicating that the powder was coarsening. This is found to be the case for many of the recycling studies found throughout the literature and is attributed to the formation of laser spatter, which is often larger than the based powder [8–10]. Although the 10th percentile of each iteration appears to be unchanging, it is noteworthy that particles below 10 µm were the most numerous in the virgin powder. As the amount of fine particles decreases, the flowability of the powder is expected to be improved since the powder becomes less cohesive due to the smaller range of particle sizes. This may explain the improvement in powder flowability observed by Tang et al. [11] as the powder is used. Future work will compare the flowability of the virgin powder to the powder after it has been used 5 times.

Although 304L laser spatter studied by the authors in previous work has been found to be typically more coarse than the base powder used in the SLM process causing coarsening as powder is recycled, its chemistry was not found to differ from virgin material with the exception of oxygen content [10]; the oxygen content of the laser spatter was measured to be 4 times greater than the

base powder. Therefore, it is expected that only the oxygen content of recycled 304L powder will increase with continual use, a claim that will be evaluated in the future. Therefore, as a preliminary step towards quantifying the change in chemistry of recycled powder, the oxygen content of several sieved -63 µm powder samples was measured with inert gas fusion at each iteration of the study. Each of the measurements conducted was repeated 3 times for a look into the variability as well. Figure 6 shows the boxplot of the oxygen content as a function of reuse. A gradual increase in oxygen content as the powder was used was observed, where the oxygen content increased from ~ 240 ppm to ~ 310 ppm. To determine if the increases in oxygen content observed were significant, ANOVA was employed with a significance level of 0.05, which yielded a p-value of less 3.2×10^{-5} indicating that the changes observed were statistically significant. To determine which measurements were different from one another, a Tukey analysis was also performed in Minitab using a significance level of 0.05. It was determined that Iteration 0 was significantly different from Iterations $2 - 5$, and Iteration 1 was significantly different from $3 - 5$. Therefore, no significant change occurred between Iterations 0 and 1. Increases in the oxygen content are commonly found by other researchers when studying recycled powder [11–13]. When looking for the source of the oxygen pickup, it is found that laser spatter ejected from the melt pool reacts with the oxygen in the chamber atmosphere while molten forming oxides. If deposited in the powder-bed surrounding parts, the total oxygen of the base material will increase as a whole, which was detected in the powder characterization performed.
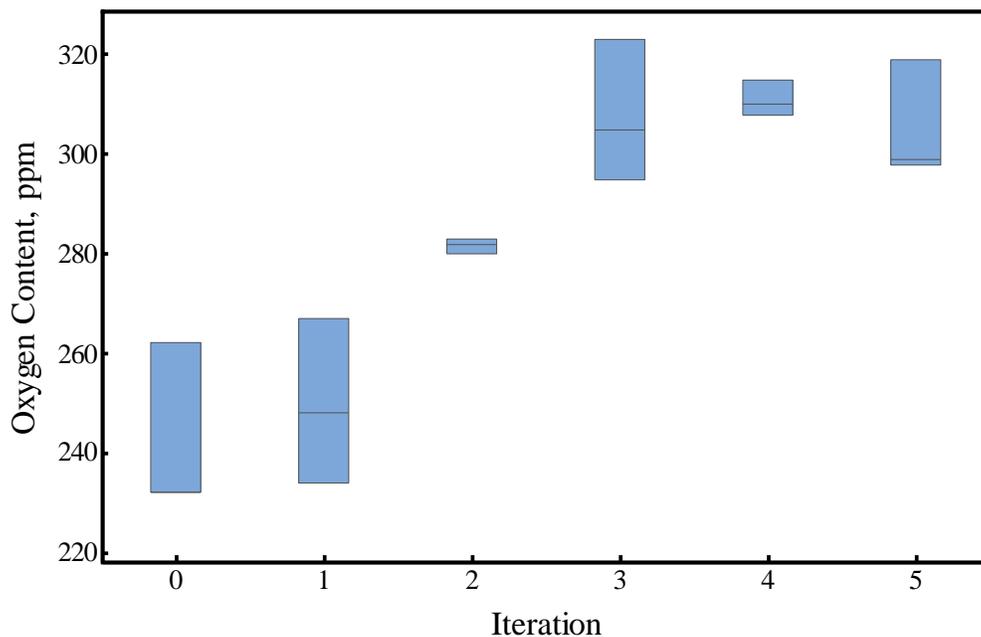

Figure 6: Boxplot of the oxygen content of powder after it is sieved at 63 µm. It can be seen that the oxygen increases with reuse.

A look at the microstructure of the recycled powder was performed with XRD. While the microstructure of powder may not play an important role in the part properties since particles will

be remelted by the laser, a change in microstructure does provide a potential means for quantifying how recycled a powder is when comparing it to the virgin state. Figure 7 shows a 3 hour XRD scan on both the unused and 5 times recycled sieved material. From the diffraction patterns, it was seen that iteration 0 powder is predominantly austenite, while powder that has been recycled 5 times reveals delta ferrite peaks. Quantification of the volume fraction of the phases present within each diffraction pattern by Rietveld refinement yield iterations 0 and 5 having 0.6% and 7.8% delta ferrite, respectively. Delta ferrite is a typical signature of laser spatter material in 304L SS as the way by which spatter solidifies is inherently different from that of virgin powder [10]. 304L is an austenitic stainless steel that follows an FA solidification mode as predicted by the chromium and nickel equivalency through the Hull expression [16]. An FA solidification mode is denoted by the following sequence of transformations:

$$L \rightarrow L + \delta \rightarrow L + \delta + \gamma \rightarrow \gamma + \delta \rightarrow \gamma$$
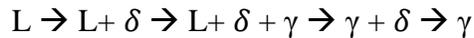
where L refers to a liquid or molten state, γ being austenite, and δ as delta ferrite. Thus, an FA solidification mode means that the material will first solidify as primary ferrite and then as austenite. Once the material solidifies, the delta ferrite phase will undergo a solid state transformation to austenite. However, as the cooling rate increases, the solid state transformation to austenite is hindered allowing delta ferrite to be retained as a metastable phase. Although it is possible that laser spatter solidifies at a higher cooling rate than gas-atomized powder, it is unlikely since laser spatter contains a significant portion of powder particles that are larger than as-received material, suggesting that many of the laser spatter particles undergo cooling rates less than that of gas-atomized powder. Since gas-atomized powder can experience cooling rates on the order of 10^5 K/s, it is possible that the melt is undercooled appreciably to solidify as primary austenite [17]. Therefore, it was hypothesized that the gas-atomized 304L powder was predominantly austenite due to the appreciable undercooling experienced during its production, whereas laser spatter does not have a sufficient amount of undercooling to solidify as primary austenite, but rather delta ferrite.
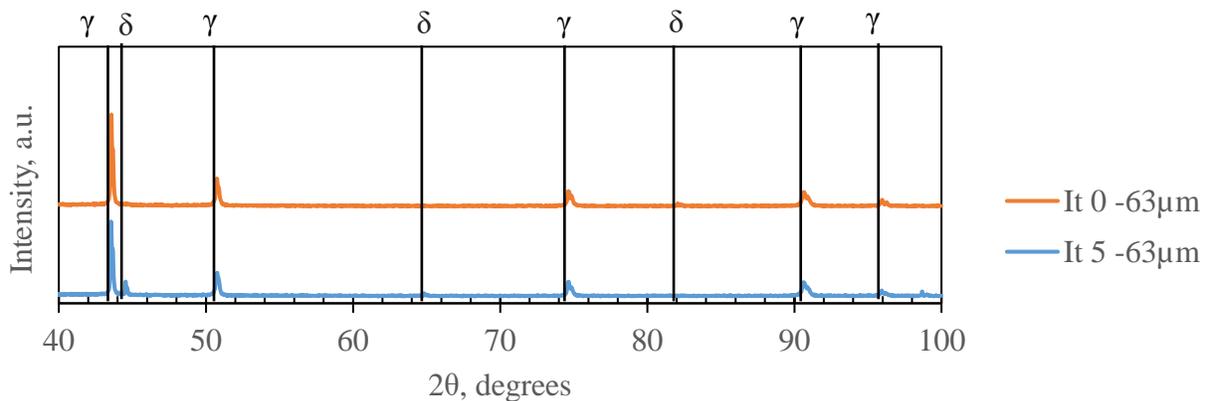
Figure 7: XRD patterns for both virgin material and powder that has been recycled 5 times. Delta ferrite was found to amount to 7.8% of the volume percentage in the used powder compared to the 0.6% in as-received material.

Part Characterization

Mini-tensile specimens were extracted from locations 1, 4, and 7 of each iteration in the recycling study to study the effect of powder reuse on tensile properties. From each location, at least 20 specimens were tested equating to at least 60 tensile specimens per iteration.
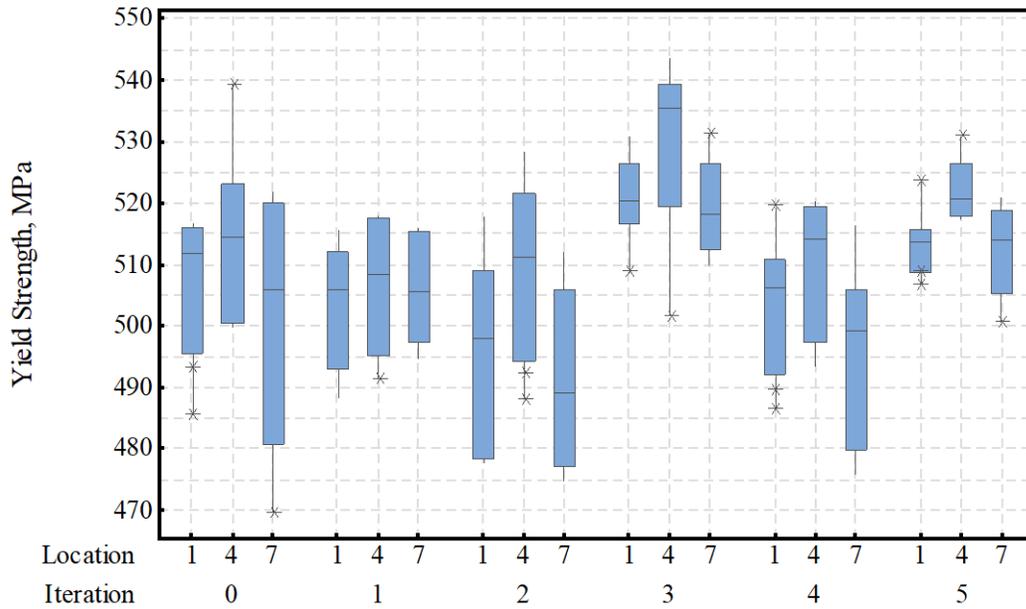
(a)
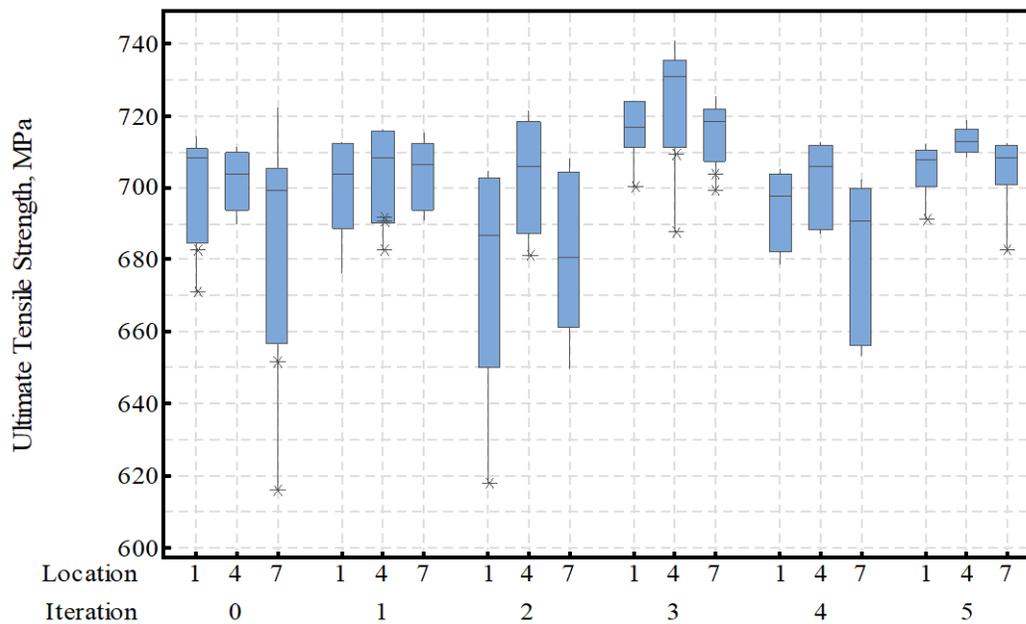
(b)

Figure 8: Boxplot of the (a) yield strength and (b) ultimate tensile strength at each iteration and location in the recycling study indicating no clear trend among the data.

Figure 8 shows both the yield and ultimate tensile strength results grouping the data in both iteration and location to better observe trends in the data. Observing the data collected on a per iteration basis, the yield and ultimate tensile strengths did not show any clear monotonic trends of decreasing or increasing strength. Moreover, any differences observed from iteration to iteration were no greater than approximately 20 MPa, which could easily be attributed to variations caused by the operator as well as inter-build differences. However, it was interesting to note that location 4 appeared to be the strongest in nearly every iteration, which pertains to the center of the build area. While this phenomenon is currently being investigated, this was believed to be a due to a slight defocusing of the beam towards the edges of the build area.

An ANOVA was performed using both the iteration and location as factors with the yield and ultimate tensile strength as responses and a significance level of 0.05. The interaction of the both the iteration and location was found to be significant with p-values of 3.7×10^{-4} and 8.8×10^{-8} pertaining to the yield strength and ultimate tensile strength data, respectively. A statistically significant interaction among the two factors means that the individual effects of iteration and location cannot be tested in regards to the effects of each on the tensile properties. Rather, the interaction among the two factors should be considered. Using a significance level of 0.05, Tukey analyses for both the yield (Table 3) and ultimate tensile strength (Table 4) revealed that iteration 3 was the strongest while iteration 2 was the weakest with the rest of the treatment combinations differing by approximately 20 MPa. While iterations 2 and 3 exhibited weak and strong tensile properties, respectively, iterations 4 and 5 are not any stronger than iteration 0. Therefore, it is again noted that no apparent trend was evident in the data. It was important to note that while statistically significant differences were computed, the practical implication of these differences was within operator error and inter-build variation as previously mentioned. If the powder is was causing differences in the tensile properties, these variations were not large enough to cause any

Table 3: Tukey analysis of yield strength comparing the interaction of iteration and location.

major concerns with respect to the yield and ultimate tensile strength. Therefore, for the specimens tested in the given locations, recycling 304L powder has no discernible effect on the yield and ultimate strength up to 5 reuses.

Iteration*Location	N	Mean	Grouping					
3 4	22	531.936	A					
5 4	22	521.266		B				
3 1	22	521.226		B				
3 7	22	519.001		B	C			
0 4	21	513.93		B	C	D		
5 1	22	513.345		B	C	D	E	
5 7	22	513.311		B	C	D	E	
4 4	22	511.47			C	D	E	F
2 4	22	510.047				D	E	F
0 1	21	509.728				D	E	F
1 4	20	508.736				D	E	F

Table 4: Tukey analysis of ultimate tensile strength comparing the interaction of iteration and location.

Iteration*Location	N	Mean				Grouping		
1 7	20	505.235	D	E	F			
4 1	22	504.94		E	F			
1 1	20	504.345			F	G		
0 7	22	503.865			F	G	H	
4 7	22	495.829				G	H	I
2 1	22	495.427					H	I
2 7	22	491.143						I

Iteration*Location	N	Mean	Grouping						
3 4	22	727.47	A						
3 7	22	717.57	A	B					
3 1	22	717.112	A	B					
5 4	22	713.066		B	C				
1 4	20	706.877		B	C	D			
5 7	22	706.434		B	C	D			
5 1	22	706.287		B	C	D			
1 7	20	704.887			C	D			
2 4	22	704.223			C	D			
0 1	21	703.81			C	D			
4 4	22	703.363			C	D			
0 4	21	702.874			C	D	E		
1 1	20	701.923			C	D	E		
4 1	22	695.665				D	E	F	
0 7	22	690.979					E	F	G
4 7	22	684.065						F	G
2 7	22	683.402							G
2 1	22	679.963							G

Conclusion

In this study, 304L stainless steel powder was recycled 5 times in the SLM process to understand the effect of evolving powder properties on the tensile behavior of as-built material. The recycling study conducted used a fixed amount of powder to accelerate powder degradation and simulate a worst-case scenario of powder reuse. Due to powder consumption for each build, the height of the build was subsequently decreased while keeping the area fraction of the build plate utilized constant. Powder characterization techniques involved the use of SEM for studying particle morphology, inert gas fusion to quantitatively examine the oxygen content, and XRD for

insight into microstructural differences between as-received and recycled powder. The differences in the observed powder properties were then evaluated for their effect on the yield and ultimate tensile strengths through testing at least 60 mini-tensile tensile specimens from each iteration of the study to increase the reliability of the data.

Morphologically, 304L coarsened with reuse with a slight change in the 10th, 50th, and 90th cumulative frequency percentiles even after being sieved through a 63 µm screen. This was due to the deposition of laser spatter in the build area during part fabrication altering the size of unconsolidated powder. While the 10th percentiles showed very little change, it was clear from the particle size distributions that reusing powder caused a subsequent decrease in the amount of particles below approximately 10 µm. Changes in the amount of fines are often accompanied with improvements in powder flowability, which will be evaluated in the future.

Chemically, recycled powder exhibited a higher oxygen content than as-received powder. In particular, the oxygen increased from approximately 240 ppm to nearly 310 ppm over the course of 5 reuses. A Tukey analysis revealed statistically significant differences between the virgin powder and the material that was recycled for 2 to 5 times. Oxygen pickup is a common occurrence when studying the reuse of material in SLM, and is due to the reaction of molten spatter solidifying in the chamber atmosphere. Although the build atmosphere was below 1000 ppm for each build in this study, Fe, Cr, Mn, and Si all react with oxygen even at low partial pressure. Consequently, oxygen pickup is inevitable for the given processing conditions.

Microstructurally, XRD was able to detect a difference between as-received and 5 times recycled powder. As-received powder was primarily austenite with 0.6% delta ferrite while the recycled powder tested contained 7.8% delta ferrite. This difference was attributed to the difference in cooling rate between the laser spatter and as-received material. Since the as-received powder was gas-atomized, its cooling rate was on the order of 10^5 K/s allowing for sufficient undercooling to develop and solidify as primary austenite. However, since laser spatter has a smaller cooling rate due to its relatively large size, it solidified as primary ferrite. Although the microstructure of the powder may not matter in SLM, crystallographic changes served as a means for discerning between virgin and recycled powder.

While changes in the powder were observed, the yield and ultimate tensile strength were not found to appreciably vary with powder reuse. Even though ANOVA and Tukey analyses showed that the differences observed are statistically significant, the changes are often no greater than 20 MPa between each iteration, which can be attributed to variations in machine setup and operator error during testing. Also important to note was the lack of monotonic trends in the data where no increase or decrease in either the yield or ultimate tensile strength was noticed. To better understand 304L recyclability, future work will entail testing of the Charpy specimens for a look into the dynamic behavior with reuse.

References

[1]   A.T. Sutton, C.S. Kriewall, M.C. Leu, J.W. Newkirk, Powder characterisation techniques and effects of powder characteristics on part properties in powder-bed fusion processes, Virtual Phys. Prototyp. 12 (2017) 3–29. doi:10.1080/17452759.2016.1250605.

[2]   J.P. Kruth, G. Levy, F. Klocke, T.H.C. Childs, Consolidation phenomena in laser and powder-bed based layered manufacturing, CIRP Ann. - Manuf. Technol. 56 (2007) 730–759. doi:10.1016/j.cirp.2007.10.004.

[3]   T.F. Murphy, Metallographic Testing of Powders Intended for Use in Additive Manufacturing, Int. J. Powder Metall. 52 (2016) 25–35.

[4]   A. Ladewig, G. Schlick, M. Fisser, V. Schulze, U. Glatzel, Influence of the shielding gas flow on the removal of process by-products in the selective laser melting process, Addit. Manuf. 10 (2016) 1–9. doi:10.1016/j.addma.2016.01.004.

[5]   B. Ferrar, L. Mullen, E. Jones, R. Stamp, C.J. Sutcliffe, Gas flow effects on selective laser melting (SLM) manufacturing performance, J. Mater. Process. Technol. 212 (2012) 355–364. doi:10.1016/j.jmatprotec.2011.09.020.

[6]   P.Y. Shcheglov, A. V Gumenyuk, I.B. Gornushkin, M. Rethmeier, V.N. Petrovskiy, Vapor–plasma plume investigation during high-power fiber laser welding, Laser Phys. 23 (2013) 016001. doi:10.1088/1054-660X/23/1/016001.

[7]   S. Ly, A.M. Rubenchik, S.A. Khairallah, G. Guss, M.J. Matthews, Metal vapor micro-jet controls material redistribution in laser powder bed fusion additive manufacturing, Nature. 7 (2017) 1–12. doi:10.1038/s41598-017-04237-z.

[8]   M. Simonelli, C. Tuck, N.T. Aboulkhair, I. Maskery, I. Ashcroft, R.D. Wildman, R. Hague, A Study on the Laser Spatter and the Oxidation Reactions During Selective Laser Melting of 316L Stainless Steel, Al-Si10-Mg, and Ti-6Al-4V, Metall. Mater. Trans. A. (2015). doi:10.1007/s11661-015-2882-8.

[9]   Y. Liu, Y. Yang, S. Mai, D. Wang, C. Song, Investigation into spatter behavior during selective laser melting of AISI 316L stainless steel powder, Mater. Des. 87 (2015) 797–806. doi:10.1016/j.matdes.2015.08.086.

[10]   A.T. Sutton, C.S. Kriewall, M.C. Leu, J.W. Newkirk, Characterization of Heat-Affected Powder Generated during the Selective Laser Melting of 304L Stainless Steel Powder, in: Solid Free. Fabr. Symp., 2017.

[11]   H.P. Tang, M. Qian, N. Liu, X.Z. Zhang, G.Y. Yang, J. Wang, Effect of Powder Reuse Times on Additive Manufacturing of Ti-6Al-4V by Selective Electron Beam Melting, Jom. 67 (2015) 555–563. doi:10.1007/s11837-015-1300-4.

[12]   L.C. Ardila, F. Garciandia, J.B. González-Díaz, P. Álvarez, a. Echeverria, M.M. Petite, R. Deffley, J. Ochoa, Effect of IN718 Recycled Powder Reuse on Properties of Parts Manufactured by Means of Selective Laser Melting, Phys. Procedia. 56 (2014) 99–107. doi:10.1016/j.phpro.2014.08.152.

[13]   J.A. Slotwinski, E.J. Garboczi, P.E. Stutzman, C.F. Ferraris, S.S. Watson, M.A. Peltz,

Characterization of metal powders used for additive manufacturing, J. Res. Natl. Inst. Stand. Technol. 119 (2014) 460–493. doi:10.6028/jres.119.018.

[14]   C.S. Kriewall, A.T. Sutton, J.W. Newkirk, M.C. Leu, Effects of Area Fraction and Part Spacing on Degradation of 304L Stainless Steel Powder in Selective Laser Melting, in: Solid Free Form Fabr. Symp., 2017.

[15]   E. Vigneau, C. Loisel, M.F. Devaux, P. Cantoni, Number of particles for the determination of size distribution from microscopic images, Powder Technol. 107 (2000) 243–250. doi:10.1016/S0032-5910(99)00192-8.

[16]   P. Korinko, S. Malene, Considerations for the weldability of types 304L and 316L stainless steel, J. Fail. Anal. Prev. 1 (2001) 61–68. doi:10.1007/BF02715336.

[17]   R.N. Wright, J.C. Bae, T.E. Kelly, J.E. Flinn, G.E. Korth, The Microstructure and Phase Relationships in Rapidly Solidified Type 304 Stainless Steel Powders, Metall. Mater. Trans. A. 19 (1988) 2399–2405.